PI Control Based DC Link Voltage Controller for Grid Integrated Domestic Photo Voltaic Systems

Nisha B Kumar
Electrical & Electronics Engg.
NITK, Surathkal
Mangalore, India
tonishabkumar@gmail.com

Jayasankar V N
Electrical & Electronics Engg.
NITK, Surathkal
Mangalore, India
jayasankarvn@gmail.com

Vinatha U
Electrical & Electronics Engg.
NITK, Surathkal
Mangalore, India
u_vinatha@yahoo.co.in

***Abstract*—The increasing energy demand and finite reserve for fossil fuel sources have led the humankind to rely on renewable energy sources. The availability of solar energy in large quantities and the increased environmental awareness among the users boosted its popularity. Grid integration of renewable source is preferred over the islanded mode of operation as there is no need for additional energy storage devices. This paper presents a proportional integral control based DC link voltage controller for grid-integrated domestic photovoltaic systems. Incremental Conductance method to extract maximum power from solar PV system, instantaneous pq theory based dual STF for fundamental component extraction, hysteresis current control method for generation of switching pulses to the inverter are the added features of this work. The grid integrated Solar PV system along with control features is modelled and simulated in MATLAB/Simulink platform. Numerical simulations are done for various system conditions. The results of the power flow study and harmonic analysis are reviewed and summarised.**

***Index Terms*—renewable energy, PV, shunt active filter, PI**

I. Introduction

The demand for energy is increasing at a faster rate due to rapid industrialization and population growth. As a result of overexploitation, fossil fuels are diminishing at a faster rate. Hence there emerges the need for replacing the fossil fuels with an alternative energy source preferably renewable energy source. Among the alternative energy sources, solar energy is one of the most abundantly available renewable energy sources. Grid integration is a means to deliver varying solar energy to the grid. The latest government policies to promote green energy has increased the use of grid-tied roof-top PV systems among domestic consumers. With the tremendous development in power electronics technology, solar PV systems can be integrated to the grid through a power electronic converter preferably an inverter. The proliferation of power electronic converters and non-linear loads at the point of common coupling (PCC) causes power quality issues in the system. The effects due to power quality issues can be alleviated by incorporating an additional feature like shunt active filtering capability to the grid interfacing converter thus reducing the overall cost of the system.

Grid-tied solar PV systems with shunt active filtering capability involves three control methods namely, maximum power point (MPPT) algorithm, a slower outer loop controller for DC link voltage control and a faster inner loop controller for harmonic current mitigation. A power converter embedded with the capability of MPPT is essential in all PV systems to ensure the best energy harvesting from the prevailing environmental conditions like varying irradiation and temperature [1]. Proportional Integral (PI) control is one of the simplest method for the control of DC link voltage. Instantaneous power theory and synchronous reference frame theory are the widely used control techniques for harmonic current mitigation [2]. A modified pq theory has been proposed for effective harmonic current mitigation under distorted and unbalanced conditions. Use of self tuning filters (STF) improves the harmonic current mitigation by eliminating the inherent phase lags introduced by conventional low pass filters [3] and [10].

According to Ministry of New and Renewable Energy (MNRE), Government of India, single phase systems are recommended for solar PV systems with peak generation upto 3 kW. In this paper a single-phase grid-tied solar PV system feeding a domestic load has been considered. The major highlight of this paper are 1) Incremental Conductance method to extract maximum power from solar PV system 2) PI control to maintain DC link voltage constant so that power flow balance is accomplished 3) Modified instantaneous theory based Dual Self Tuning Filter for harmonic current mitigation 4) Hysteresis current control used for generation of switching pulses of the inverter switches. The single-phase voltage and current values are transformed to an equivalent two phase frame, for implementing the instantaneous power theory. The performance of the double-loop control system for different system conditions is validated using numerical simulations in MATLAB/Simulink platform. The paper is organized as follows: Section II discusses the detailed description of the overall system including the MPPT algorithm employed, section III gives control system description, section IV presents the simulation results and section V concludes the paper.

II. System Description

The overall system consists of a distribution grid feeding a single-phase non linear load to which the PV system is integrated using a single-phase shunt connected voltage source inverter.The circuit diagram of the overall system is shown

978-1-5386-8190-9/19/$31.00 ©2019 IEEE

in Fig. 1. The following subsections describe the various components involved in detail.

A. Solar PV system

The elementary unit of a PV system is the solar cell. Cells are assembled to form modules and modules are grouped to form large PV arrays. Solar PV system comprises of PV arrays joined in series and in parallel. The solar PV system is represented as a current source generating I_m [4] as given in (1) and (2) .The equivalent circuit of solar PV system [4] is given in Fig. 2.

$$I_m = N_p I_{cell} - N_p I_o exp^{[\frac{\gamma}{N_S V_t a}-1]} - [\frac{\gamma}{R_p(\frac{N_s}{N_p})}] \quad (1)$$

where

$$\gamma = V_{PV} + I_{PV} R_s(\frac{N_s}{N_p}) \quad (2)$$

I_m, the model current, V_{PV}, the the terminal voltage of PV system, I_{PV}, the terminal current, I_o, the saturation Current, V_t, the thermal voltage, N_s, the number of arrays connected in series, N_p , the number of arrays connected in parallel, I_{cell},the photovoltaic current of the PV cell, a, the Diode constant,R_s, the series resistance of the array,R_p, the shunt resistance of the array.

B. MPPT Algorithm

The power generation in the PV system largely depends on changing irradiation and temperature conditions. In order to extract maximum power from the PV system, the terminal voltage and current are to be maintained at maximum power points (MPP). The IV and PV characteristics of solar PV at variable insolation and at constant temperature of 25^oC are respectively given in Fig. 3 and Fig. 4.

1) Incremental Conductance Method: The incremental conductance method utilizes the slope of the PV array power characteristics to track the MPP. The flowchart for the incremental conductance method [1] is as given in Fig. 5.

C. Boost Converter

The output voltage generated by the solar PV system is varying with respect to varying solar irradiation and temperature. The variable DC voltage is converted to fixed DC using dc-dc boost converters. The output of dc-dc boost converters is connected to the DC link. Boost converter design equations [5] are shown in (3) and (4).

$$\frac{V_{ob}}{V_{inb}} = \frac{1}{1-D} \quad (3)$$

$$L_b = \frac{D(1-D)^2 R_b}{2f_s} \quad (4)$$

where, V_{ob} = Output voltage (V), V_{ib} = Input voltage (V), D = duty ratio, L_b = Inductance (H), R_b = Load resistance (Ω), and f_s = Switching frequency (Hz).

D. Voltage Source Inverter

A single phase H-bridge voltage source inverter (VSI) with IGBT switches and antiparallel diodes is used in this system. The VSI interconnects the solar PV system to the grid and mitigates current harmonics at the distribution grid.

E. DC link capacitor

DC link capacitor is used for decreasing the dc ripple. Larger the DC capacitor value, smaller the ripple. If P_{dc} , V_{dc} and C_{dc} represent the power available at the DC link, DC link voltage and DC link capacitor, DC capacitor value can be obtained as [6] as given in (5).

$$C_{dc} = \frac{P_{dc}}{2\omega V_{dc} \Delta V_{dc}} \quad (5)$$

The DC link voltage V_{dc} [6] is given in (6)

$$V_{dc} = 1.25\sqrt{2} v_s \quad (6)$$

F. AC filter Inductor

AC filter is used to filter out the undesirable switching frequency components from the inverter current. The filter inductance can be calculated using (7) where, h is the hysteresis band, fs, the switching frequency,

$$L_f = \frac{V_{dc}}{4hf_s} \quad (7)$$

III. Control System

This section explains the design of the control system for the grid interfacing inverter. The control system incorporates two loops, an outer voltage control loop and an inner current control loop. The functions of the control system are (i) to maintain the dc link voltage constant and balance the power flow, (ii) to compensate the harmonic components of the load current at PCC. PI controller is used for implementing the outer loop of the control system. The inner loop of the control system uses the instantaneous p-q theory. STF is employed in the inner loop to extract the fundamental component of load current and grid voltage.

A. Design using PI controller and instantaneous power theory

The schematic diagram of the PI controller based control system is shown in Fig. 6.

1) Outer loop design: In the outer loop, DC link voltage is sensed and an error signal based on energy difference is processed through PI controller [7]. The block diagram representation of DC voltage regulator is shown in Fig. 7.

The transfer function is of the following form as shown in (8).

$$\frac{V_{dc}^2}{V_{dcref}^2} = 2\zeta\omega_n \frac{s + \frac{\omega_n}{2\zeta}}{s^2 + 2\zeta\omega_n s + \omega_n^2} \quad (8)$$

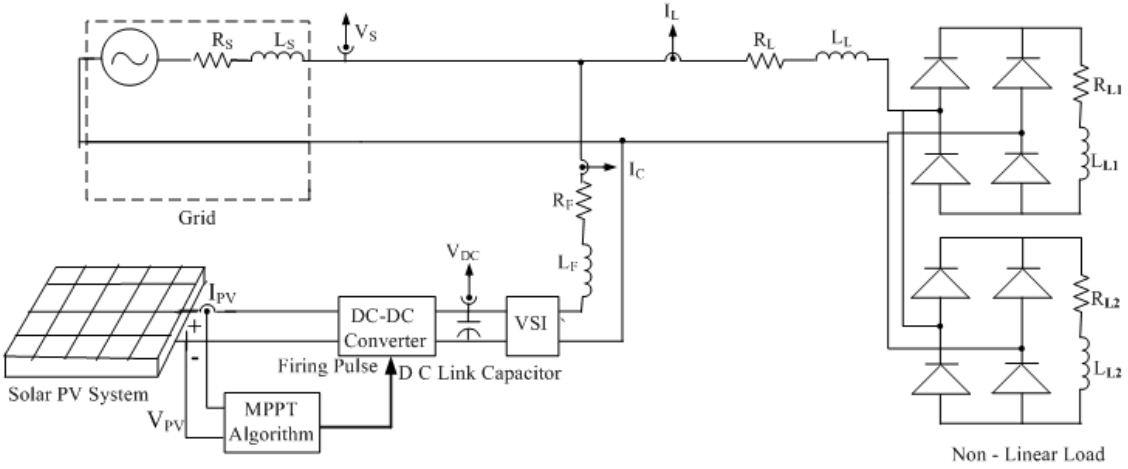

Fig. 1. Schematic diagram of a grid tied Solar PV system feeding non-linear load at load center

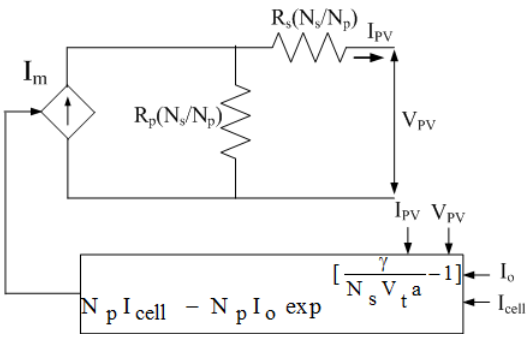

Fig. 2. Equivalent Circuit of Solar PV System

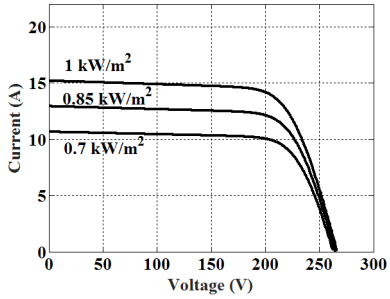

Fig. 3. IV characteristics of Solar PV System at variable insolation and at constant temperature of 25^oC

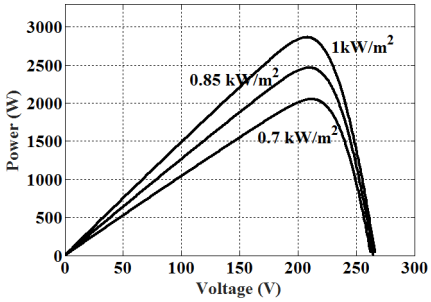

Fig. 4. PV characteristics of Solar PV System at variable insolation and at constant temperature of 25^oC

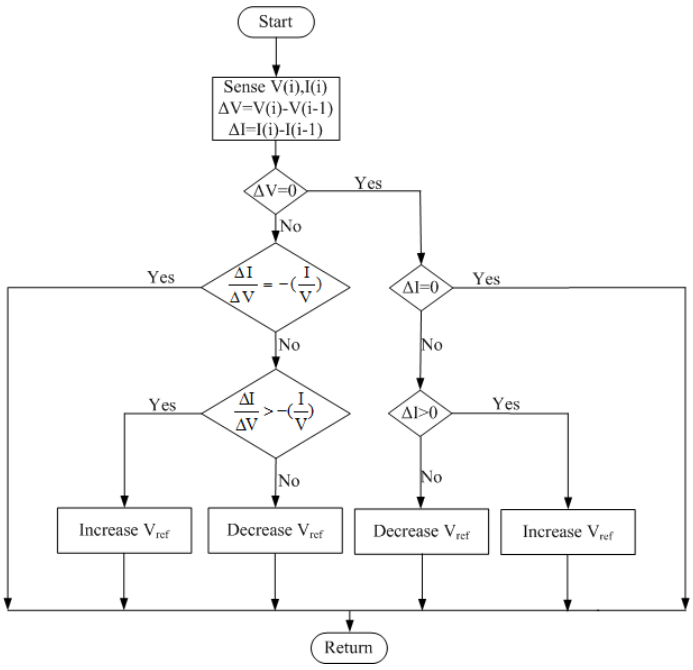

Fig. 5. Flowchart for Incremental Conductance Method

where ω_n and ζ are natural frequency of undamped oscillations and damping constant of PI controller respectively. Proportional and integral constants can be derived from the transfer function as in (9).

$$k_p = 2\zeta\omega_n C, k_i = \omega_n^2 C \tag{9}$$

Ps, the output of the PI controller represents the power provided by the network to preserve the charge in the DC link capacitor.

2) Inner loop control: The inner loop control is based on instantaneous pq theory [8] and [11].The load current and grid voltage are sensed and transformed to $\alpha\beta$ frame using (10) and (11) where i_L and v_s are the load current and the grid voltage

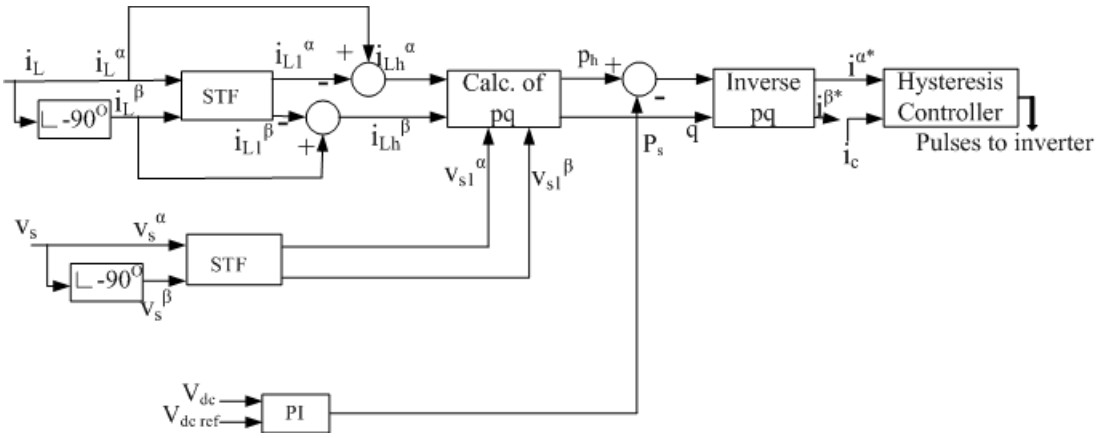

Fig. 6. PI based control system

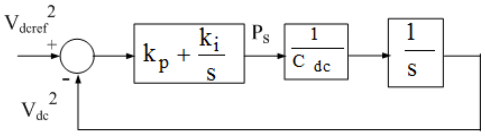

Fig. 7. Block Diagram of DC voltage regulator using PI controller

respectively. i_L^α, i_L^β and v_s^α, v_s^β are the load currents and grid voltages in $\alpha\beta$ frame.

$$i_L^\alpha = i_L \angle 0, i_L^\beta = i_L \angle -90 \tag{10}$$

$$v_s^\alpha = v_s \angle 0, v_s^\beta = v_s \angle -90 \tag{11}$$

The fundamental component of load current and grid voltage are determined using the self tuning filter (STF). The schematic diagram of STF is shown in Fig. 8. The mathematical model of STF is given by (12) and (13),where, K is the sensitivity parameter of STF and ω_1, the fundamental frequency.

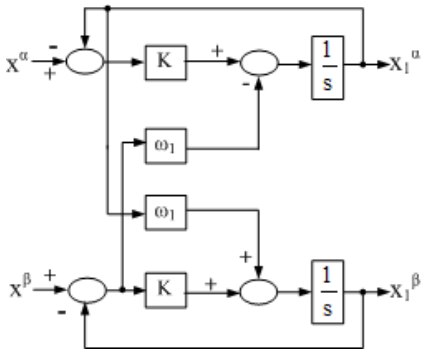

Fig. 8. Schematic diagram of STF

$$x_1^\alpha(s) = \frac{K}{s}[x^\alpha(s) - x_1^\alpha(s)] - \frac{\omega_1}{s}x_1^\beta(s) \tag{12}$$

$$x_1^\beta(s) = \frac{K}{s}[x^\beta(s) - x_1^\beta(s)] - \frac{\omega_1}{s}x_1^\alpha(s) \tag{13}$$

Instantaneous real power needed for harmonic compensation, and instantaneous imaginary power needed for reactive power compensation are calculated using (14) and (15). The negative sign indicates that the power flow direction is from inverter to PCC .

$$p_h(t) = -(i_{Lh}^\alpha v_{s1}^\alpha + i_{Lh}^\beta v_{s1}^\beta) \tag{14}$$

$$q(t) = -(i_L^\beta v_s^\alpha - i_L^\alpha v_s{}^\beta) \tag{15}$$

The power calculated in the outer loop, P_s is added with the instantaneous real power needed for harmonic compensation $p_h(t)$, and the reference currents for compensation are calculated using (16), where $K_{\alpha\beta} = (v_{s1}^\alpha)^2 + (v_{s1}^\beta)^2$.

$$\begin{bmatrix} i^{\alpha*} \\ i^{\beta*} \end{bmatrix} = \frac{1}{K_{\alpha\beta}} \begin{bmatrix} v_{s1}^\alpha & -v_{s1}^\beta \\ v_{s1}^\beta & v_{s1}^\alpha \end{bmatrix} \begin{bmatrix} p_h + P_s \\ q \end{bmatrix} \tag{16}$$

The reference current is then compared with the inverter current i_c and the gating signals are generated using hysteresis control [9]. The working of hysteresis controller is illustrated using Fig. 9.

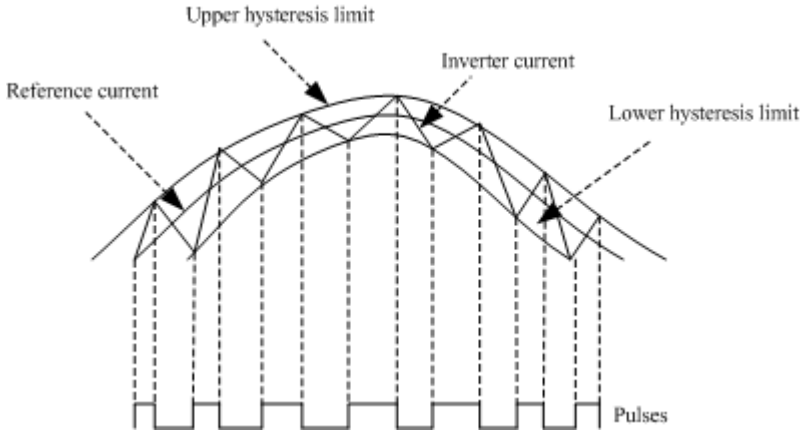

Fig. 9. Gating signal generation using hysteresis control

IV. Results

Numerical simulations are done using MATLAB/Simulink platform. Both steady state and dynamic conditions are considered for testing the performance of the controller.The rated generation of solar PV system is $2880W/m^2$. The daily load profile of the consumer and the daily solar irradiation profile for the consumers location in the month of March are shown in Fig. 10 and Fig. 11 respectively. The system specification is as in TABLE. I

TABLE I
System Specification

Sl. No	Particulars	Values
1	Grid Voltage	1Φ, 230 V (RMS), 50Hz
2	Source Parameters	0.01mH, 0.1 Ω
3	DC link capacitance	2350 μF
4	DC link voltage	390 V
5	Filter Parameters	5mH, 0.1 Ω
6	Solar PV specification	open circuit voltage 22.2V and short circuit current 7.5 A

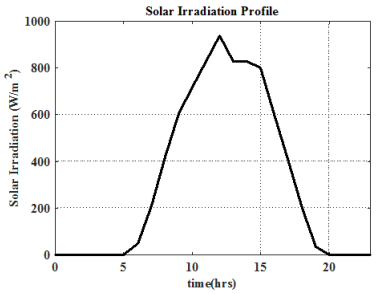

Fig. 10. Solar irradiation profile

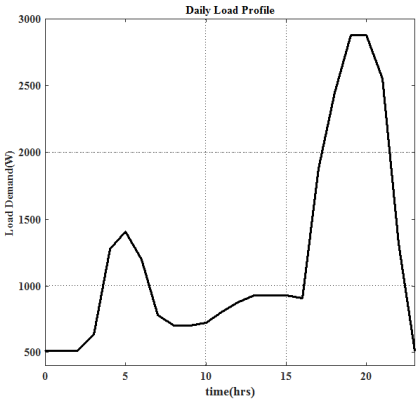

Fig. 11. Daily load profile

A. Steady State condition

1) Case 1:Constant solar irradiation and load demand with undistorted grid: A constant irradiation of 830 W/m^2 and 930W load demand at 13-14 hours is choosen for simulation study as given in Fig. 10 and Fig. 11. It is observed from Fig. 12 that DC link voltage is retained at 390 V. The grid current, compensation current and load current waveforms for case1 are shown in Fig. 13, Fig. 14 and Fig. 15 respectively. As excess power is injected to the grid, the grid current will be 180^o out of phase with the grid voltage . The load demand is met by the active power generated by the solar PV system and the excess power is injected to the distribution grid as given in Fig. 16. The THD of the grid current is 2.64% which is within the limits specified by IEEE 519 as given in TABLE. II.

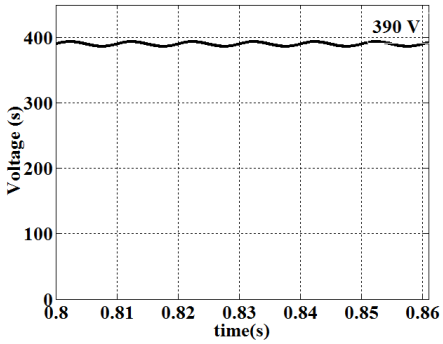

Fig. 12. DC Link Voltage case 1

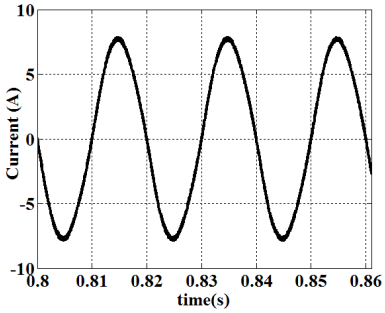

Fig. 13. Grid Current case 1

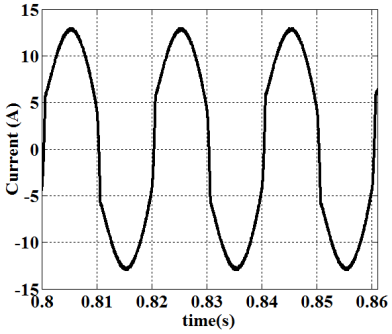

Fig. 14. Compensation current case 1

2) Case 2:Constant solar irradiation and load demand with distorted grid : A constant irradiation of 830 W/m^2 and 930W load demand at 13-14 hours is choosen for simulation study as given in Fig. 10 and Fig. 11. A grid voltage distortion of 3% is simulated by injecting 2.2% fifth order and 2% seventh order voltage harmonics into the grid. It is observed from Fig. 17 that DC link voltage is maintained at 390 V. The grid current, compensation current and load current

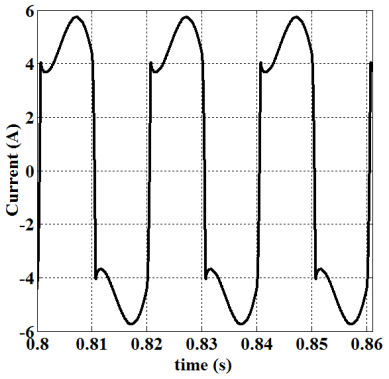

Fig. 15. Load current case 1

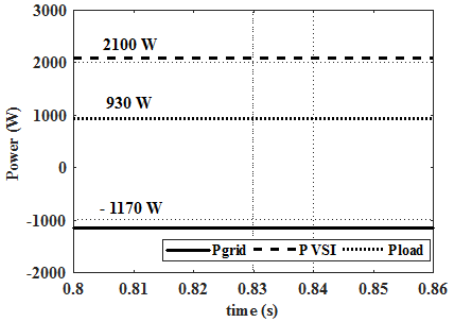

Fig. 16. Active Power case 1

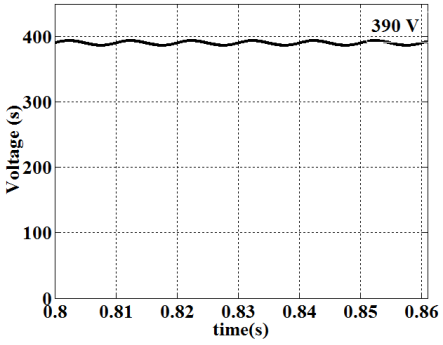

Fig. 17. DC link Voltage case 2

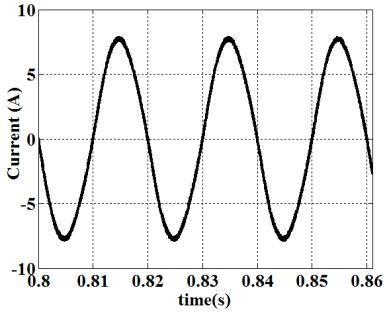

Fig. 18. Grid Current case 2

waveforms for case 2 are shown in Fig. 18, Fig. 19 and Fig. 20 respectively. As the surplus power is injected to the grid, the grid current will be 180^o out of phase with the grid voltage. The load demand is met by the active power provided by the solar PV system and the excess power is injected to the distribution grid as given in Fig. 21. The THD of the grid current is 3.43% which is within the limits specified by IEEE 519 as given in TABLE. II.

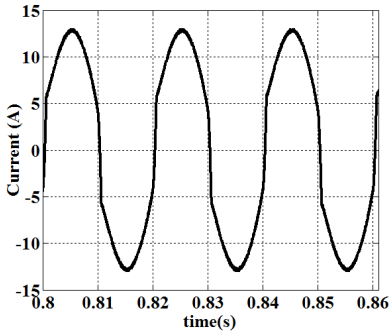

Fig. 19. Compensation Current case 2

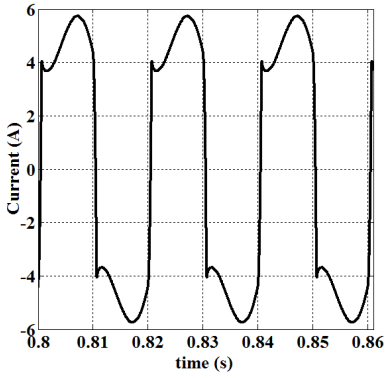

Fig. 20. Load Current case 2

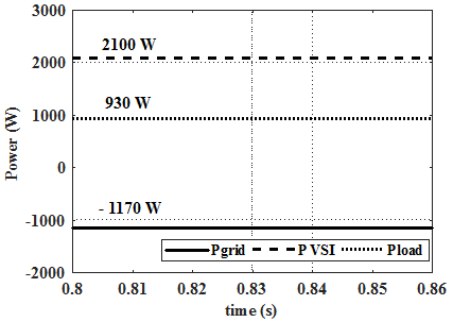

Fig. 21. Active Power case 2

B. Dynamic Condition

1) Case 3: Constant load varying solar irradiation: A constant load of $930W$ is considered in this case. A step change in solar irradiation from $800W/m^2$ to $600W/m^2$ is applied at 1 s. This condition is at 14-15 hours in Fig. 10 and Fig. 11. The DC link voltage waveform for case 3 is shown in Fig. 22 which demonstrates that DC link voltage is

retained at 390 V.The grid current, compensation current and load current waveforms for case 3 are as in Fig. 23, Fig. 24 and Fig. 25 respectively. The active and reactive power plots for case 3 are shown in Fig. 26 and Fig. 27. During dynamic condition the controller acts in such a way that the power flow balance is maintained between VSI, grid and the load. As excess power is injected to the grid, the grid current will be 180^o out of phase with the grid voltage. The THD of the grid current after attaining steady state after dynamic condition is 2.07% which is within the limits specified by IEEE 519 as given in TABLE. II

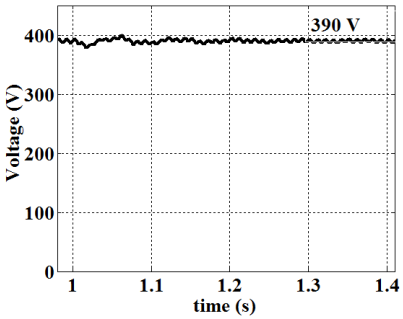

Fig. 22. DC link Voltage case 3

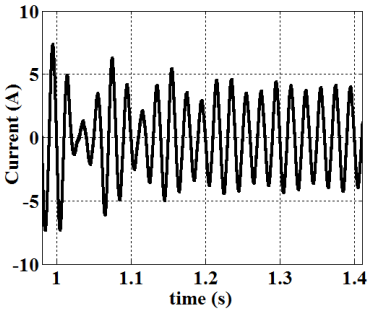

Fig. 23. Grid Current case 3

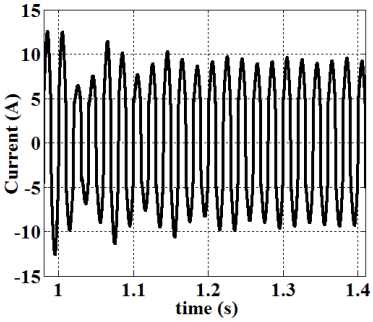

Fig. 24. Compensation Current case 3

2) Case 4:Constant solar irradiation varying load: A step change in load from 910W to 1600W applied at 1s under constant solar irradiation of $800W/m^2$ is considered here. The DC link voltage is preserved at 390 V as can be observed in Fig. 28. The grid current, compensation current and load current waveforms for case 4 are shown in Fig. 29, Fig. 30 and Fig. 31 respectively. The active and reactive power plots for case 4 are shown in Fig. 32 and Fig. 33 respectively.

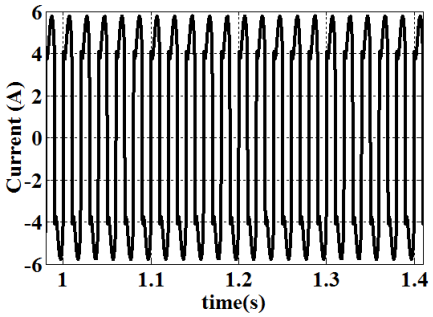

Fig. 25. Load Current case 3

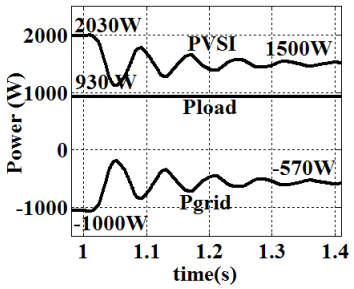

Fig. 26. Active Power case 3

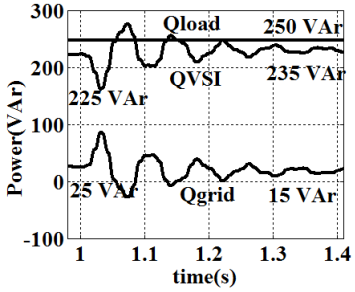

Fig. 27. Reactive Power case 3

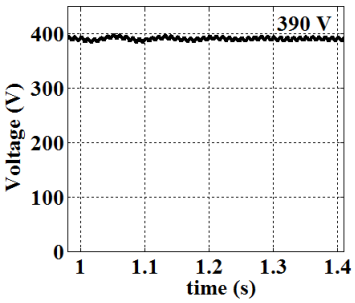

Fig. 28. DC link voltage case 4

During dynamic condition the controller acts in such a way that the power flow balance is achieved between VSI, grid and the load. As surplus power is injected to the grid, the grid current current will be 180^o out of phase with the grid voltage. The THD of the grid current after attaining steady state after dynamic condition is 4.92% which is within the limits specified by IEEE 519 as given in TABLE. II.

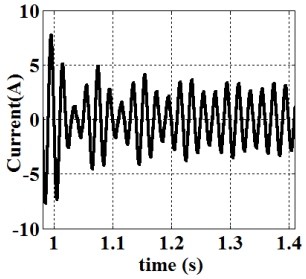

Fig. 29. Grid Current case 4

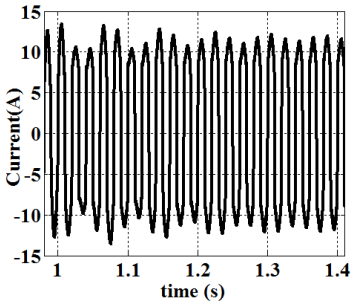

Fig. 30. Compensation Current case 4

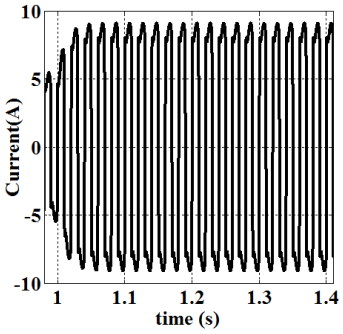

Fig. 31. Load Current case 4

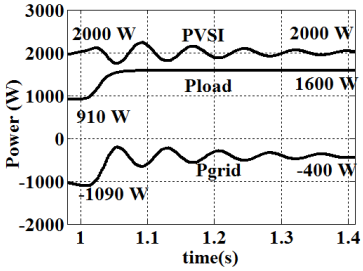

Fig. 32. Active Power case 4

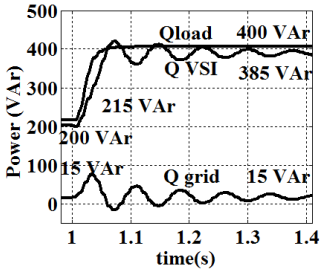

Fig. 33. Reactive Power case 4

TABLE II
THD (%)

Condition	Case	Grid Voltage	Grid Current	Load Current
Steady State	1	0	2.64	34.11
Steady State	2	3	3.43	35.03
Dynamic	3	0	2.07	35.03
Dynamic	4	0	4.92	38.72

V. Conclusion

A single phase domestic level grid-tied PV system with shunt active power filter functionality has been modelled, simulated and analysed. A dynamic model of PV system with MPPT features is connected to the DC link of single phase VSI through a DC-DC boost converter. The single phase grid voltage and load current are transformed to a pseudo two-phase system using instantaneous theory. A harmonic current mitigation loop using STF based PQ theory and a DC-link voltage control loop using PI Controller have been designed and simulated. From the numerical simulation studies conducted using MATLAB/ Simulink platform, the performance of the controller under steady state and dynamic conditions is found to be effective.The controller not only controls the power flow in the system based on the system changes , but also maintains the grid current THD within 5 % limit as recommended by IEEE standard-519.

References

[1] H. Rezk and A. M. Eltamaly,“A comprehensive comparison of different MPPT techniques for photovoltaic systems,” Journal on Solar Energy(Elsevier), volume.112, Jan. 2015, pp.1–11 .

[2] H. Akagi, Y. Kanazawa, and A.Nabae, “Instantaneous Reactive Power Compensator Comprising Switching Devices Without Energy Storage Components,”IEEE Trans. Ind. Appl., vol. IA-20, 1984, pp.625–630.

[3] M. A. Salam, P. Poure and S.Saadate, “ Hardware implementation of a three-phase Active Filter system with harmonic isolation based on Self-Tuning-Filter,” IEEE Power Electr. Conf., Aug. 2008, pp. 2276–2278.

[4] M.G. Villava, J. R.Gazoli and E. R. Filho, “ Comprehensive Approach to Modeling and Simulation of Photovoltaic Arrays,” IEEE Transactions on Power Electronics, vol. 25, May 2009, pp.1198 – 1208.

[5] H. A. Mohamed, H. A. Khattab, A. Mobarka and G. A. Morsy, “Design, control and performance analysis of DC-DC boost converter for stand-alone PV system,” Eighteenth International Conf. (MEPCON), 2016.

[6] S. Biricik, S. Redif, S. K. Khadem and M. Basu, “ Improved harmonic suppression efficiency of single-phase APFs in distorted distribution systems, ” Int. Journal of Electronics, vol.103, 2016 , pp.232–246.

[7] M. K. Mishra and K. Karthikeyan, “ A fast acting dc link voltage controller for three phase dstatcom to compensate ac and dc loads,” IEEE Transactions on Power Delivery, vol.24, 2009, pp. 2291–2299.

[8] V.Khadkikar, A. Chandra and B. N. Singh,“Generalised single phase p-q theory for active filtering:simulation and dsp based experimental investigation,” IET Power Electronics, vol.2, pp.67–78, 2009.

[9] Z. Chelli, R. Toufouti, A. Omeiri and S. Saad, “ Hysteresis Control for shunt active power filter under unbalanced three phase conditions,” Journal of Electrical and computer Engineering,vol.15, 2015.

[10] S.Biricik , S. Redif, O. C.O zerdem, S. K. Khadem and M. Basu, “Real-time control of shunt active power filter under distorted grid voltage and unbalanced load condition using self-tuning filter, IET Journal on Power Electronics, vol.7, issue. 7, pp.1895 – 1905, 2014.

[11] P. S. Magdum and U.T. Patil,“Development of Single Phase Shunt Active Power Filter”,International Conference on Inventive Communication and Computational Technologies (ICICCT 2017), 2017